STUK-YTO-TR 211 / OCTOBER 2004

FOCUSED MODELLING

Fracture identification in Olkiluoto borehole OL-KR04

Jarkko Jokinen, Kai Jakobsson

STUK • SÄTEILYTURVAKESKUS
STRÅLSÄKERHETSCENTRALEN
RADIATION AND NUCLEAR SAFETY AUTHORITY

Osoite/Address • Laippatie 4, 00880 Helsinki
Postiosoite / Postal address • PL / P.O.Box 14, FIN-00881 Helsinki, FINLAND
Puh./Tel. (09) 759 881, +358 9 759 881 • Fax (09) 759 88 500, +358 9 759 88 500 • www.stuk.fi

The conclusions presented in the STUK report series are those of the authors and do not necessarily represent the official position of STUK.

ISBN 951-712-911-4 (print, Dark Oy, Vantaa/Finland 2004)
ISBN 951-712-912-2 (pdf)
ISSN 0785-9325

JOKINEN Jarkko (Geological Survey of Finland), JAKOBSSON Kai. Focused modelling. Fracture identification in Olkiluoto borehole OL-KR04. STUK-YTO-TR 211. Helsinki 2004. 33 pp.

Keywords: nuclear waste, Olkiluoto site, site characterization, focused modelling, PCA analysis, geophysics, borehole method, fracture section

Abstract

An extensive set of measured borehole data has been obtained from geological repository investigations in the bedrock of Olkiluoto. Our hypothesis is that geophysical data may be used more efficiently to identify and classify fracture zones. It is known that several geophysical logging methods yield useful information outside the borehole walls that cannot be reached otherwise. At present, this data is used for additional fracture characterization but not for identification purposes.

The study focuses on the application of 14 different geophysical data measured in the borehole OL-KR04. The whole data set is divided into main groups using the Principal Component Analysis (PCA). Each group is composed mainly of sensitive methods detecting specific physical characteristics. The main groups from the geophysical point of view are open fractures, reduced density, increased electrical conductivity, and increased natural radiation. The Varimax optimization method is used to maximize the importance of supporting data as well as to emphasize differences between the discovered principal components.

In fracture zone analysis, drilling core samples and the hydrological measurement results form an indispensable data set. For practical reasons, and in order to fulfill the requirements of the PCA analysis, S-wave velocity and electrical resistivity measurements are also performed. A combination of these methods, simultaneously applied using suitable “trigger limits”, identifies penetrated extensive fracture sections in a borehole cost-effectively and unambiguously.

JOKINEN Jarkko (Geologian tutkimuskeskus), JAKOBSSON Kai. Kohdennettu mallinnus. Rikkonaisuusrakenteiden tunnistus Olkiluodon kairareiästä OL-KR04. STUK-YTO-TR 211. Helsinki 2004. 33 s.

Avainsanat: ydinjäte, Olkiluodon loppusijoitusalue, loppusijoitusalueen ominaisuuksien tunnistus, kohdennettu mallinnus, PCA-analyysi, geofysiikka, poranreikämenetelmä, rakovyöhyke

Tiivistelmä

Tarkasteltaessa Olkiluodossa tehtäviä kallioperätutkimuksia on havaittu, että jo toteutettuja geofysikaalisia poranreikämenetelmiä olisi mahdollista hyödyntää aikaisempaa enemmän rikkonaisten jaksojen paikantamisessa ja laadun arvioinnissa. Tyypillisesti aineistoa on käytetty rikkonaisuusrakenteiden lisäominaisuuksien ja varmuusluokan määrittämiseen. Useat geofysikaaliset mittausmenetelmät tarjoavat kuitenkin hyödyllistä lisätietoa reikien läheisestä kallioperästä sekä rikkonaisten jaksojen jatkuvuudesta.

Tutkimuksessa on rajoituttu kairanreiästä OL-KR04 kerättyyn 14 erilaiseen mittausaineistoon. Aineisto jaettiin pääkomponenttianalyysillä (PCA) erilaisia kallioperän fysikaalisia ominaisuuksia tunnistaviin ryhmiin. Tärkeimmät ryhmät ovat avoimet raot (raoissa vettä), alentunut tiheys, kohonnut sähkönjohtavuus sekä kohonnut luonnon radioaktiivinen säteily. Aineiston tilastollisessa pääkomponenttianalyysissä käytettiin Varimax-optimointia, jolloin keinotekoiset mittaustulokset edustavat mahdollisimman hyvin kutakin ryhmää. Käytetty menetelmä korostaa samalla näiden pääkomponenttien eroavaisuuksia.

Kallioperän rikkonaisuuden tutkimuksessa välttämättömiä aineistoja ovat kairasydännäyte sekä vedenjohtavuuden vaihtelu reiässä. Pääkomponenttianalyysiin ja käytännön soveltamiseen perustuva täydentävä aineisto on S-aallon nopeuden ja kallion näennäisen ominaisvastuksen muodostama kombinaatio. Näiden kolmen menetelmän avulla tunnistetaan kustannustehokkaasti ja yksiselitteisesti rakotihentymät, joilla on selkeä jatkuvuus reiän ulkopuolisessa kalliotilavuudessa.

Contents

ABSTRACT 3

TIIVISTELMÄ 4

1 INTRODUCTION 7

2 DATABASE 9

3 MEASURING DEPTH 10

4 BOREHOLE OL-KR04 DATA 12
4.1 Sampling 12
4.2 Background corrections 13

5 PCA ANALYSIS 15
5.1 Rotation and factors 16
5.2 Data restrictions 21
5.3 Results of PCA 22

6 IDENTIFICATION METHODS 25
6.1 Trigger limits 25
6.2 Combination of data 26
6.3 Identification in OL-KR04 27
6.4 Method combination 30

7 CONCLUSIONS 32

REFERENCES 33

1 Introduction

The Finnish Radiation and Nuclear Safety Authority (STUK) supervises the geological investigations of the final disposal facility for spent nuclear fuel at the Olkiluoto study site. After surface and borehole investigations in the area, the study site location is defined and the characterization (access) tunnel excavation begins. The ca. 5 km long spiral tunnel will penetrate numerous different kinds of geological features including fracture zones. Hydraulic fracture zones are unsuitable details that have to be avoided when spent nuclear fuel canisters are to be placed down into the rock mass. The drilling and borehole information obtained along the access tunnel excavation work may be used for testing and improving predictive methods of detecting important features before the tunnel excavation reaches the area. A reliable prediction method is invaluable when planning excavation of storage tunnels for spent nuclear fuel canisters.

The co-operation between the Geological Survey of Finland (GTK) and STUK on focused modelling has continued for several years. Markku Paananen has analyzed available borehole data collected from a limited bedrock volume at the Olkiluoto study site (Paananen 2001). "Trigger limits" were defined for several geological, geophysical, and hydrological parameters and used in fracture zone interpretation. The bedrock in the modelled volume was typically slightly fractured with generally gently-dipping fractures. A total of 23 fracture zone sections were detected in four boreholes penetrating the 500 m × 500 m × 200 m study volume. Attention was paid to the description of fracturing and the estimation of potential crosshole connections on the basis of observed fracture properties, borehole radar, and seismic VSP results. However, only a few potential connections between the detected fracture zones were located.

The next project focused on the same study volume, but this time an attempt was made to define a simple parameter combination with trigger limits to select and classify important fracture zone sections in the boreholes (Jokinen and Jakobsson 2002). The reported values for fracture frequency, slickenside fractures, loss of core, and fracture zones were used simultaneously with pre-processed geophysical resistivity and acoustic data. Fracture zone observations were interpreted individually. Fractured zones between boreholes were not combined.

An earlier classification of geological modelling also applied the Principal Component Analysis (PCA) (Korkealaakso et al. 1994) and hydrological data, but the PCA was later abandoned. Posiva Ltd's latest bedrock model (version 2003/1, Vaittinen et al. 2003) introduces three main classes: fractured or crushed zone (R), hydraulic feature (H) and a combined class (RH). Exceeding the "trigger limit" of hydraulic conductivity identifies a hydraulic feature. It is measured with 2 m long measuring gauge.

It has been noticed that visual core sample classification does not always coincide with the engineering classification in use. Visual classification is descriptive and divides the samples basically into fracture zones and intact rock. Rock classified as intact is considered suitable for disposal of spent nuclear fuel. In tunnel excavation work, efforts are made to avoid fracture zones as much as possible. What happens in marginal cases where fracture zone criteria are not met but the rock mass seems to have poor quality all the same?

An earlier PCA analysis produced an artificial measurement result, which was used in selection of fracture zones. The PCA in Korkealaakso et al. (1994) was performed using five data sets that were available at the moment. The selected loggings were not the best possible and the selection was changed in further applications. The method was not used for restricting the number of data sets through the creation of principal components, but rather

for finding the statistically most typical behavior of the used information. Fracture density was always selected as a data set although it was also used independently as a criterion in the fracture identification process. The first principal component was used as a result in the applied Factor Analysis in Posiva's bedrock model version 2001/1.

The fracture zone characterization system used in the bedrock model version 2003/1 (Vaittinen et al. 2004) is based on core samples and down-hole results of hydraulic conductivity measurements combined with borehole TV. Other rock and fracture properties outside the boreholes are not taken into account. If a fracture does not leak, the identification of the fracture section in question is based solely on an engineering-geological core classification (Gardemeister et al. 1976, Korhonen et. 1974).

When a borehole penetrates a section of diverging rock properties, the section can often be seen in geophysical loggings. Various specific methods have been developed for detecting the different properties and the instruments' usability depends on the requirements. This work focuses on analyzing different geophysical logging methods and the aim of the study is to recommend a set of methods that provides useful supplementary information for fracture identification purposes and classification systems.

One of the aims of this work is to develop new alternative fracture zone detection and classification systems based on the Olkiluoto borehole data. The method should meet several demands simultaneously: **1)** the results should coincide better with visual observations based on general impressions instead of an engineering classification, **2)** the method should be simple and logical to apply, and **3)** the method should give an interpretation result rapidly after measurements. These requirements may prove essential when an underground rock-characterization facility tunnel (ONKALO) work is going on and the pilot holes are available only for a very short time before the tunnel excavation continues and reveals how successful the rock structure and fracture zone prediction was. Later, a workable method could be used for disposal tunnel predictions.

2 Database

This work utilizes Posiva's TUTKA database. The database is collected from the Olkiluoto study site and contains geological core logging information, drilling parameters, measured geophysical surface and borehole data, results of hydrological pumping tests, etc. The database has been collected during the long study period started in 1984. The older data in the database is not outdated, but more accurate or more effective methods have replaced the old ones; totally new investigation methods have been developed or taken into use, and, similarly, some of the older methods have been left behind. The old geophysical borehole loggings were carried out with contemporary equipment that may not exist today. The available resources were redirected more appropriately owing to acquired knowledge or changed interest. Data collecting methods were changed whenever necessary. However, the new data has been measured using more recent methods and the old data was measured using the old methods. Therefore, the data sets from different boreholes are not equal.

The geophysical logging is carried out with equipment hanging at the end of a winch cable. The borehole probes and cables vary widely in type. The winch cables have an important role in geophysical logging because the measured information includes two parameters: the measured result and the measured location. Both parameters should be correct before the data is really useful in this kind of a detailed investigation.

Without knowledge of the correct measuring depth, the different borehole loggings are possibly unreliable for comparison in a fracture analysis. A penetrated fracture zone is typically a relatively short section in a borehole. An important hydrological connection may be several centimetres thick. If we accept a 0.2 % inaccuracy in depth results, it results in ±1 m accuracy at the investigation depth of 500 m. There is a high risk of obtaining a data set without overlapping geophysical anomalies from a given fracture zone. A fracture analysis is a much more detailed study than traditional prospecting with large-scale ore bodies.

3 Measuring depth

Geophysical data consists of a measured rock property and its location. The correct depth is crucial when different borehole data sets are analyzed together. However, a typical borehole study at the site is carried out without real time in-situ controlled depth calibration of the used instrumentation. As an exception, there are borehole probes that are able to measure several rock properties simultaneously in which case the results form accurately overlapping data sets.

When data sets are compared using Factor Analysis, the goodness of the result depends on the quality of the original data. Fig. 1 represents an example where the PCA is calculated from two almost similar data sets. This example shows what happens when the data sets are not overlapping at the end of the borehole. The distance coordinate from the surface (depth) of the other data set is slightly stretched to obtain a linearly increasing shift between the data sets. On the left in Fig. 1, the data sets overlap. Here, the first principal component dominates and the second component is insignificant. An increasing shift between the data sets results in the PCA analysis shown on right in Fig 1. The first component, PCA1, consists of two low peaks that may not be significant when sections are selected from the principal components of the borehole data.

The winch cable may become strained, when the measuring probe is lowered down. If the probe touches the bottom of the borehole, the exact location of the probe is known (the typical boreholes in Olkiluoto are open to the bottom and their depths are known). If a faulty measuring / probe location is identified, the depth values along the borehole should be corrected. Before a successful depth correction can be performed, the behavior of the probe's displacement along the borehole needs to be known. Typically, a correction is performed on the basis of assumptions instead of calibration. The first assumption is that displacement increases linearly from surface to bottom, but however, it is more probable that the behavior is not linear. Inaccurate depth values are produced for several different reasons.

Cable strain is an individual characteristic of

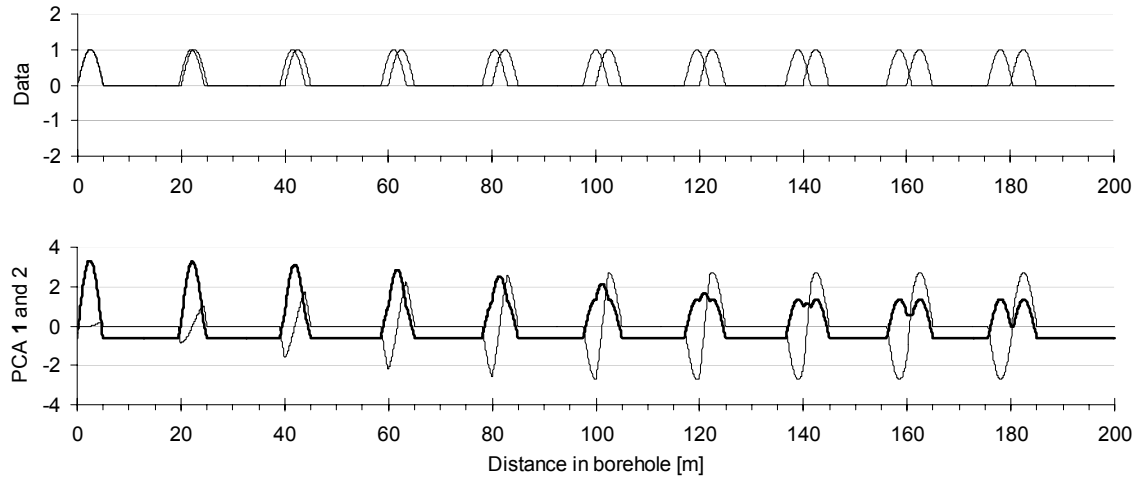

Figure 1. PCA analysis of two data set results PCA1 (bold) and PCA2 (thin).

different measuring systems. At least the probe's weight, the specific weight of the cable, cable materials and structure, as well as time-dependent properties have an effect on cable strain. However, strain may be a minor component causing incorrect depth values. In addition, dipping angle, slipperiness of borehole wall, and measuring direction (moving direction up or down) have an effect. Saline water shows different buoyancy at different depths in the boreholes of Olkiluoto. Increased amounts of saline water (deeper) result in higher density and provide increased buoyancy for probe and winch. In addition, the temperature differs and varies typically on the surface and in the borehole, which also causes a potentially slow transformation in the winch cable when it is lowered down into the borehole.

One common source of location inaccuracy is the tripod wheel. The user has to check at least that the circumference of the wheel and the radius of the winch cable are compatible, that the contact between the cable and the wheel is non-slip - also when the winch motor is started and stopped. The user also has to check that the winch cable comes straight to the wheel to ensure the instrument's acceptability for use. A natural assumption is that the surface elevation (Z=0) is always chosen correctly.

Another simple assumption used in strain correction is that strain is linearly dependent on tensile strength: double strength causes double strain. This assumption is useful when the cable in use is marked for calibration. The total weight of the hanging winch cable and probe together M [kg] is:

$$M = AZ + B,$$

where A is specific weight of cable [kg/m], Z is uncoiled cable length [m] and B is probe weight [kg]. Cable strain (ΔZ) is $\Delta Z = CM$, where C is an extension factor of the cable [m/kg]. For uncoiled cable, total strain (ΔZ_{TOT}) is

$$\Delta Z_{TOT} = C\int_0^Z (AZ + B)dZ = C(\frac{1}{2}AZ^2 + BZ),$$

where the cable's specific weight (A) has an important role if there is no upper limit of strain. The bottom of the borehole is a suitable test point where the location of the probe end (Z) and total strain (ΔZ_{TOT}) are accurately known. Probe weight (B) and the cable's specific weight (A) are also known parameters. An extension factor can be derived from the previous equation

$$C = \Delta Z / (\frac{1}{2}AZ^2 + BZ).$$

Cable strain is probably at its highest when the cable is new and it is uncoiled for the first time. Part of the strain is irreversible. Therefore, cable strain may vary from year to year. Eventually, the cable does not become further strained and all cable stress ends up on the winch. Cable material and structure may prevent strain after a maximum value. Strain may increase partly fast and partly slowly, wheel problems may disappear after the cable is opened enough, etc. A wide range of wild cards in depth measuring has to be accepted, but the correct depth values are required anyway.

Location corrections along the borehole could be made afterwards. Due to individual variation in rock properties, geophysical anomalies produced by the different methods do not necessarily come from the same location and the form and width of the anomalies may also vary. However, using visual comparison it is possible to identify, estimate, and correct the shift caused by different methods. The correction may be linear as when associated with the wheel problems, or non-linear when potentially associated with cable strain, etc. One practical method to ensure correct depth data is using artificial depth marks inside the borehole. It should be possible to detect the marks with all used methods.

4 Borehole OL-KR04 Data

The study is focused on the 900 m deep borehole OL-KR04 owing to its central location. The planned ONKALO access tunnel will be excavated close to OL-KR04. The borehole is expected to represent quite well the surrounding rock showing typical fracturing and hydrological features.

Many geophysical and other borehole loggings have been carried out in OL-KR04. The borehole was drilled in two phases (0–503.20 m in 1989 and 503.20–901.58 m in 1995). Part of the data sets consists of two parts with overlapping sections, but also some complete duplicates have been measured. The most recent deviation measurements carried out in the borehole extend only to the depth of –700m and differ from the original deviation data to such an extent that they have not been used in this study. One of the most useful data is the core-logging data (Niinimäki 2004). Rock and fracture properties are analyzed and they form the basis of the rock and fracture zone classifications. The comparison of the geological data from the surface and all boreholes to each other is used for structuring a geological model of the area.

Core sample data is useful, but it does not contain all data that boreholes provide. Geophysical measurements and hydrological tests gain information from outside the boreholes. Certain methods like tubewave attenuation and borehole diameter measurements are directed inside the borehole walls. Some methods, like gamma radiation, P-wave velocity, and susceptibility, extend the study range outside the borehole to the adjacent surrounding rock. Hydrological conductivity, fluid temperature (including the effects of inflow), and rock resistivity measurements are influenced by a large volume outside the borehole, including a fracture net between the borehole and the surface.

In this work there are fourteen different data sets used in the Principal Component Analysis. The data is presented in Table I.

Table I. Borehole data of OL-KR04 applied in this work.

1	P-wave velocity
2	Tube wave attenuation
3	S-Wave velocity
4	Rock resistivity
5	Resistance
6	Waterflow
7	Caliber
8	Susceptibility
9	Hydrological conductivity
10	Gamma radiation
11	Gamma scattering
12	Gamma attenuation
13	RQD
14	Fracture frequency

Some of the measured borehole data has not been used because of problematic utilization or because the measurements focus only on short sections instead of the whole borehole OL-KR4. For example, fluid temperature, fluid resistivity, galvanic charged potential, seismic VSP-reflection, hydrological pumping tests, and drilling parameters are not included in the PCA work.

4.1 Sampling

All data is interpolated to a 0.05-m sampling distance. When the original data has coarse sampling density, new points are interpolated linearly between the old points. When the original data has been denser, the new values are calculated linearly from the nearest points and the rest of the data is abandoned. When the data is measured from a specified section instead of a point, all generated points every 0.05 m inside the sections have received the same value without linear interpolation. This kind

of an increase of data density has been performed on the hydrological conductivity data.

The depth values of some of the data have been corrected visually. The magnetic susceptibility data from the surface to the bottom of the borehole OL-KR04 consists of two data sets with a 20-m overlap at the depth of 480–500 m. The first data set is measured erroneously from the surface to the depth of 505.39 m (borehole depth 503.2 m). The depth correction is carried out by using a clear magnetic anomaly detected in the second data set (measured from 480 m to 900 m) at the depth of 488.4 m. The corresponding anomaly in the first data set is located 4.75 m deeper. The depth values of the first data set are linearly corrected to obtain the anomaly on the other.

The rock resistivity data consists of two data sets as well. The first and the second data sets have a 20-m overlap at the depth of roughly 480–500 m. A detected distinct resistivity anomaly has a 3.1-m depth difference in the two data sets. The first data set is linearly corrected (stretched) to obtain the anomaly at the same depth in both data sets. Later, the uniform data set is linearly corrected to fit the anomalies to the same places as in the other borehole data. The corrections are based on fracture data combined from core samples.

Minor linear depth correction is performed also on the depth values for the rock resistance and tube wave attenuation data. The correction includes a small shift and linear strain throughout the borehole. The corrected anomalies fit better with the other data sets including the fracture frequency and RQD data.

Fracture density is calculated using a 1-m detecting window with a 0.05-m moving distance (moving average). This work applies the TUTKA database where fracture location is based on core sample analyzes. Fracture mapping using borehole image data has been carried out. It has a more accurate and natural database, but the study focuses only on two sections, namely 385–485 m and 456–745 m (Tammisto et al. 2002).

4.2 Background corrections

The effects of the variable borehole temperature and fluid conductivity are corrected using the original resistivity and resistance data. However, slow depth-dependent variation in electrical conductivity of saline fluids changes the background level of resistivity and resistance measurements. Corresponding anomalies of similar geological structures at different depths reach different maximum values due to the background level. This skews data distribution and misinforms potential correlation with the other borehole data. Unprocessed resistivity and resistance data cannot be used in the PCA analysis.

The background of the resistance and resistivity data is visually estimated (Figs. 2 and 3) and removed from the original data. Background levelling generates comparable data from all depths and removes wrong correlations with other borehole data.

Figures 2 and 3 present the resistivity and resistance data measured in OL-KR04. Fit background variation is removed from the original data to produce residual variation. The residual data is used in the PCA work.

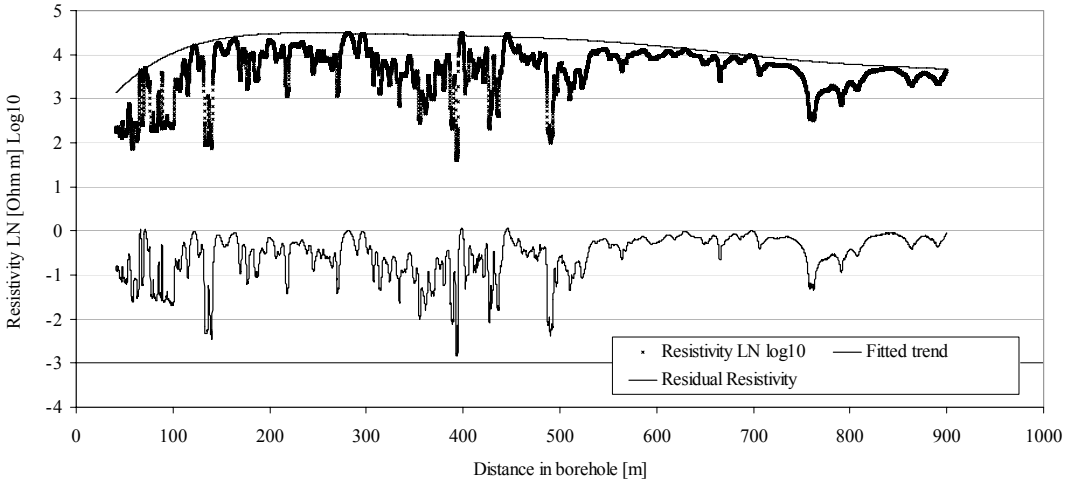

Figure 2. Background variation of resistivity data is removed to make separate anomalies comparable.

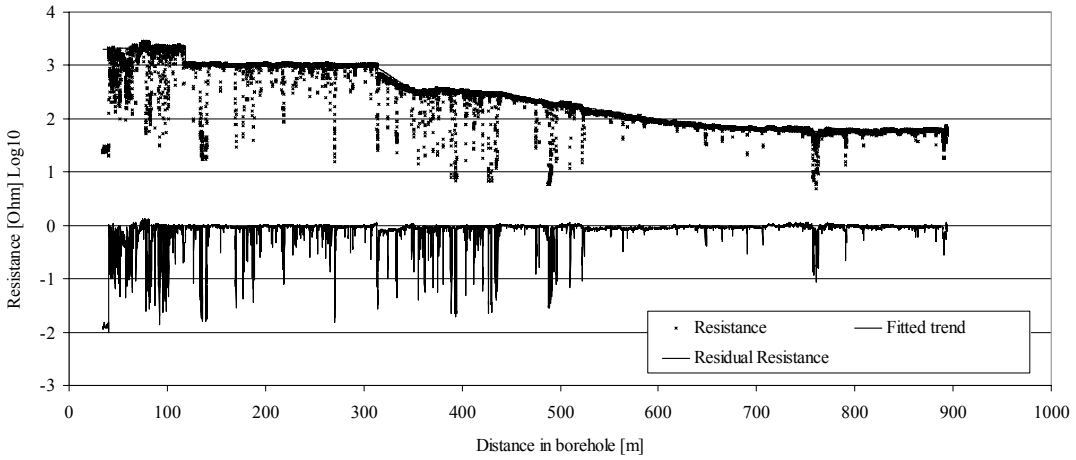

Figure 3. Background variation of resistance data is removed to make separate anomalies comparable.

5 PCA analysis

Factor Analysis is primarily used for data reduction or structure detection. The purpose of data reduction is to remove redundant (highly correlated) variables from the data file, perhaps replacing the entire data file with a smaller number of uncorrelated variables. The purpose of structure detection is to examine the underlying (or latent) relationships between the variables.

In Factor Analysis, the original data is transformed into a new orthogonal system. The maximum variation of the data is explained by the first principal component – illustration P1 in Fig. 4. The second component (P2) explains the rest of the original variation. The data distribution in the new components P1 and P2 is scaled to give an average of 0 and a standard deviation of 1.

The PCA method is a statistical method and statistical adequacy has to be ensured. The original data from OL-KR04 is measured typically from the depth of about 40 m downwards, but due to the hydrological conductivity measurements, the common data set begins at the depth of 100 m. The studied depth section (103.7–893.7 m) includes 15,801 data points with a 0.05-m sampling interval (with decent readings of hydraulic conductivity, the data point number is 13,399, explained later).

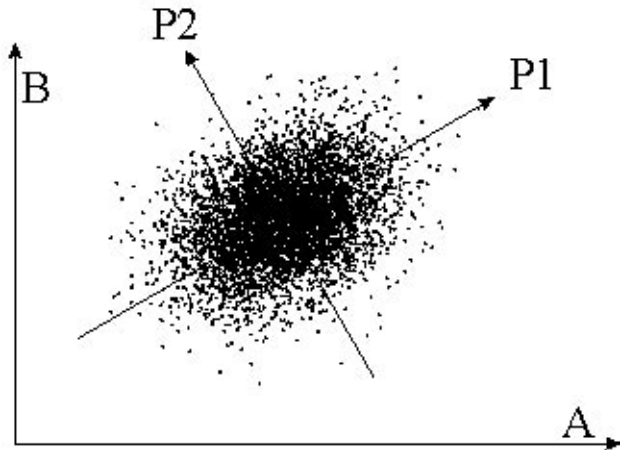

Figure 4. Data A and B show slight correlation. The PCA process sets new origin and axes to clarify the behavior of the original data.

The borehole is regionally representative, but, naturally, complete data from all the boreholes would cover the area better. It takes time to find out what kind of a combination of borehole and method forms the most representative data set. The full spectrum of different methods is not applied in all the boreholes.

When a normal PCA is calculated, the result consists of one or more principal components with weighting values for all original data sets. The number of the original data sets and the number of explained components are equal, but only a number of the most important components are selected to explain the main variation. The ignored minor components include noise and occasional variation. The most important components are called principal components. The first principal component P1 is formed according to the behavior of the majority of the data. The data that correlates with the general behavior gets a high weighting value (positive or negative) in the analysis of P1. A data set with low correlation with the general variation gets a weighting value close to zero. Next, the principal components in Factor Analysis are calculated similarly. The component is formed on the basis of the typical behavior of the rest of the variation, and also in orthogonal direction with respect to the first component, etc.

The PCA makes all methods even and the attitude of interpretation is clearly mathematical. However, geophysical methods measure different kinds of rock properties that may show direct or indirect correlation, or no correlation at all. All geophysical methods have a relatively constant importance in the PCA analyses and when the majority of the selected methods are sensitive to the presence of open fractures, also the first principal component detects sections of open fractures. Therefore it is expected

that P1 will strengthen the idea formed on the basis of core samples and gives only trivial amounts of new information. From this point of view, also the other principal components are important if they have some kind of a physical connection with the appearance of fractures or weakness zones in the rock mass. An important fracture zone may be penetrated by drillings, but its fractures are closed or filled or, by contrast, the borehole has penetrated a very local detail that has no continuity. Other borehole methods provide additional information that is not obtained from the calculations of P1.

It is possible to restrict the number of principal components. The simplest way is to pick only the first component. P1 represents the most typical data behavior – not the joint effect of all data. When the number of PCA components is not restricted, also the geophysical grip is preserved. If new data does not support previous principal components, a new principal component is added and explained statistically. All accepted principal components are statistically essential for explaining variation in the original data. Unimportant variation is abandoned automatically.

5.1 Rotation and factors

This work applies rotation in Factor Analysis. Combination of the data of the different principal components was chosen in order to maximize the significance of the supporting data. The orientation of the P1 axis is rotated into an optimal direction to increase the importance of the consistent data. Data of small importance to the rotated component does not affect the calculation of the orientation of the axis. Further, P2 and the other orthogonal components are also rotated to find an optimized data base and direction. The optimization process increases the components' physical differences. In addition, rotation makes important data groups more equal, as shown in Table III.

The number of principal components is set freely as it is required by the input data. The data results in five different main components P1–P5 presented in Table II. Electrical resistivity and resistance are background corrected to obtain depth independent data. Also the magnetic susceptibility and electrical resistivity data are depth corrected as presented previously. The hydrological conductivity and water flow data are in their original form.

The PCA result in Table II shows that the data is simplified to five significant variables. The principal components (factors) P1–P5 have clear explanations as to how they are formed from the original data. The factor P1 is supported by RQD, S-wave, fracture frequency, P-wave, tube wave, and quite well also by the borehole caliber measurements. If one single method ought to be chosen to represent this component, it would be RQD owing to its highest value in the group. The first component calculated in the PCA process is the strongest and it explains 24% (32 % without optimization) of all variations as shown in Table III.

Table II. Principal Component Analysis of borehole data OL-KR04 100–900 m (15801 depth points, 14 data sets). Rotated Component Matrix(a).

	Component				
	P1	P2	P3	P4	P5
pwave	.744	.437	.130	–.054	.128
tubew	.594	–.218	.095	–.181	.306
rrty	.327	–.001	.652	.005	.253
rrce	.159	.034	.861	–.046	.020
wflow	–.008	–.036	–.008	*.869*	.024
calib	–.503	–.048	–.098	–.032	.171
susc	.091	–.235	–.786	.001	.091
hydr	–.098	.027	–.026	*.861*	–.005
ngam	.091	–.098	–.063	–.038	–.907
gamma	.214	.885	.139	–.008	–.003
gamre	.196	.893	.099	.006	.082
swave	.818	.260	.123	–.140	.125
rqd	.826	.132	.034	.026	-.080
frac	–.781	–.137	–.028	.024	.089

Extraction Method: Principal Component Analysis.
Rotation Method: Varimax with Kaiser Normalization.
Rotation converged in 5 iterations.

The second component is mainly supported by the different gamma scattering measurements. The component is slightly stronger than the third component (P3) compiled from the resistivity, resistance, and susceptibility data. The fourth component (P4) combines the hydrological measurements, and the last component (P5) is almost the same as the original natural gamma radiation as shown in Table II.

The five major components together explain 70% of all variation of the borehole data. The other minor components together, a total of nine, explain the rest, i.e. 30%, of all variation. An important detail is that each of the original data sets supports some of the selected five main principal components (Tables II and III).

Table III. Summary of the main components of the borehole data of OL-KR04. Total Variance Explained.

Component	Initial Eigenvalues			Extraction Sums of Squared Loadings			Rotation Sums of Squared Loadings		
	Total	% of Variance	Cumulative %	Total	% of Variance	Cumulative %	Total	% of Variance	Cumulative %
1	4.427	31.622	31.622	4.427	31.622	31.622	**3.311**	23.652	23.652
2	1.630	11.643	43.265	1.630	11.643	43.265	**1.931**	13.790	37.442
3	1.461	10.434	53.699	1.461	10.434	53.699	**1.925**	13.749	51.191
4	1.250	8.931	62.630	1.250	8.931	62.630	**1.520**	10.861	62.052
5	1.004	7.171	69.800	1.004	7.171	69.800	**1.085**	7.749	69.800

Extraction Method: Principal Component Analysis.

The rotation of the P1–P5 is based on the Varimax method (Harman 1976, Reyment and Jöreskog 1993). The data used for each rotated component is chosen to obtain as pure components as possible. The efficiency of the rotations is illustrated in Fig. 5. Relative component loading before (blue) and after (yellow) rotation shows that the rotation increases notably the load of the strongest components. The consequence of the rotation is that the components are constructed using the most suitable data, not using a common average.

The first component P1 is composed mainly of core information and acoustic data. The borehole diameter has a minor role and ca. 50% of its variation is explained by P1. The result concludes that the acoustic data supports the core data, but also vice versa. The S-wave velocity provides the best acoustic compatibility with P1. The example section

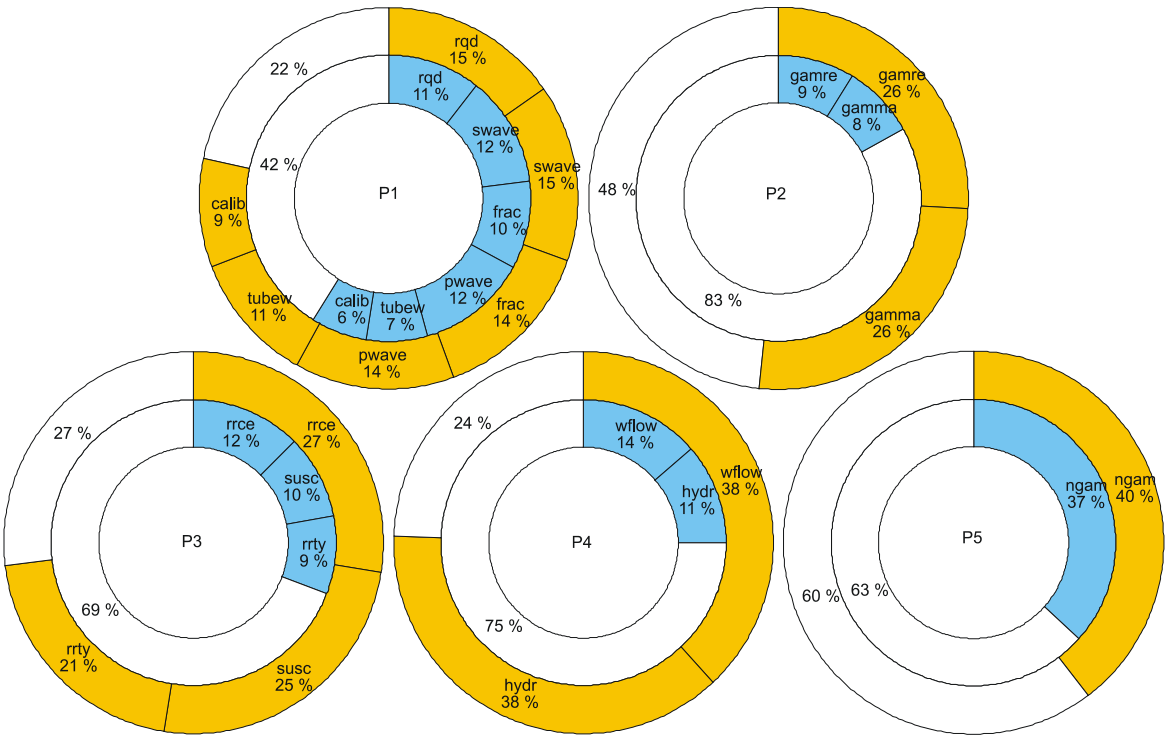

Figure 5. Component loading. The blue color describes the portion of the most valuable borehole data for each component P1–P5 when factor axes are not optimized. The yellow colour describes the data account after rotation. The white slice describes the relative portion of the minor data sets together.

data that forms P1 is presented in Fig. 6.

The variation of P1 resembles considerably the reported fracture zones in OL-KR04 (Fig. 6) between 500 m and 550 m. The drilling report (Rautio 1995) states that there is a fracture structure of class RiIII-IV between the depths of 522.45 m and 524.00 m (blue highlighting in Fig. 6). The section between the depths of 522.75 m and 524.00 m is crushed into small particles including a 0.15-m core loss section. The crushed zone with the core loss explains the local minimum between two high fracture frequency peaks in the highest curve (frac) of Fig. 6. In this kind of a section, the user of the data may set fracture frequency at the highest level in order to avoid interpretation problems in the automatic calculation systems. The section between 505.89 m and 507.00 m (yellow in Fig. 6) is classified into the structure class RiIII and is detected with the S-wave measurements as well. This zone is not clearly detected by the tube wave or P-wave measurements. However, the section close to 510 m (green in Fig. 6) is detected with all measuring instruments used, but it is not mentioned in the drilling report. The previously reported structures in the selected section are presented in Table IV. The section close to the depth of 510 m is located inside the old structure detected between 506.5–526.5 m (R17B, Vaittinen et al. 2001), but it remains outside the last interpretation determined between 522.22–524.22 m (KR04_7R, Vaittinen et al. 2003).

Table IV. Reported core loss and fracture class determinations of the section 500 m – 550 m of OL-KR04 (Rautio 1995)

Depth, m	Core loss, m	Fracture class
505.89–507,00		RiIII
522,45–524,00		RiIII-IV
522,75–524,00	0,15	crushed sample

The geophysical data presented in Fig. 6 as well as the principal component P1 presented in Fig. 7 suggest that the section close to 510 m has properties corresponding to the fracture structure of KR04_7R (522.22–524.22 m). The drilling sample may not be representative there. This example shows that the S-wave measurements may be the most useful and efficient borehole method for detecting open fracture structures in the boreholes of Olkiluoto.

The factors P1–P5 along the same borehole OL-KR04 section 500–550 m are presented in Fig. 7. The figure shows that the component P1 has much higher anomalies than the other factors. This is a local characteristic and the variation is levelled out

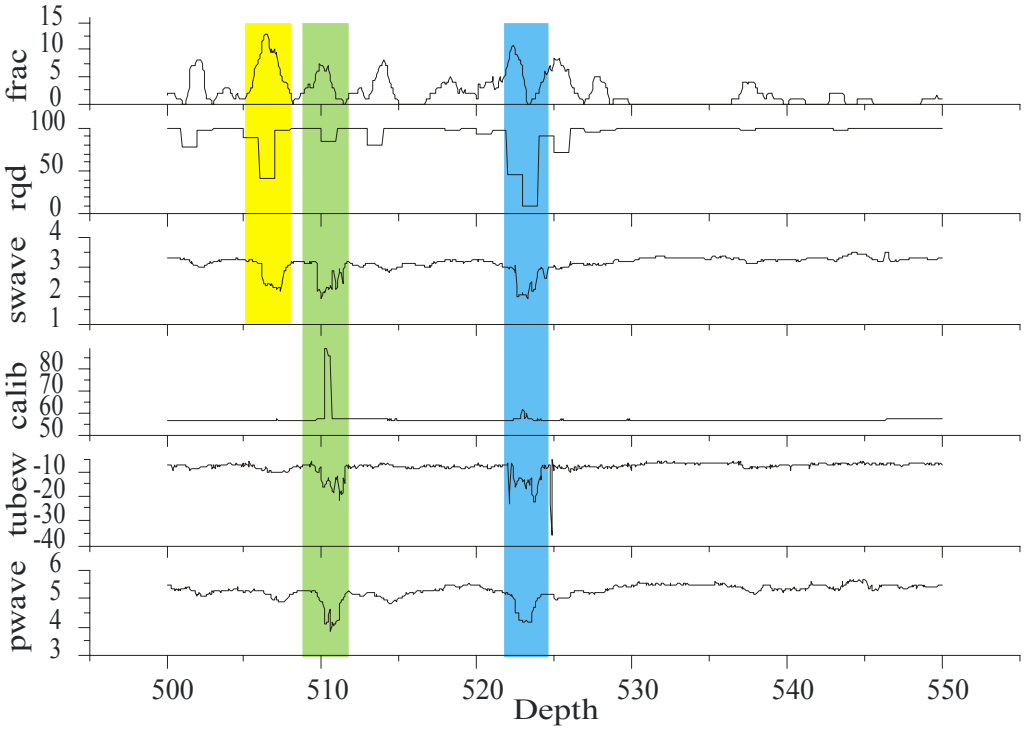

Figure 6. Selected data from the OL-KR04 borehole, distance between 500 m and 550 m. The PCA component P1 is composed of the fracture frequency (frac, 1/m), RQD (rqd), S-wave (swave, km/s), caliber (calib, mm), tube wave attenuation (tubew, dB/m), and P-wave velocity (pwave, km/s) data.

to normal distribution (0±1) when observing the principal components of the entire borehole.

Open (fluid filled) fractures form the physical background to and explanation of P1. Drilling may open fractures close to the borehole and increase detection possibilities by geophysical methods. Open fractures are easy to detect from core samples and the results have also direct effect on the RQD classification. Open fractures contain water that prevents the S-wave and slows down the travel of the P-wave. The broken borehole wall resulting from open penetrated fractures increases tube wave attenuation.

The value of P1 varies between –15 and 4 on the total length of the borehole OL-KR04. The anomalous sections form strong and sharp negative peaks. The behavior of P1 makes it a suitable factor for detecting and defining fractured structures.

The produced P1 is based on 14 different borehole data with valuable support from 6 different loggings. The component agrees well with fracture frequency, RQD, acoustic data, and borehole caliber. P1 is like a "summary" of this supportive data. However, P1 does not represent all analyzed data; it is only a combination of a restricted, strongly correlated data set. The PCA result includes the other principal components as well.

The factor P2 consists of gamma scattering and the gamma scattering relation of far and near distance (radiometric attenuation). The behavior of P2 is quite variable, but very high peaks do not occur as shown in Fig. 8. The variation is restricted

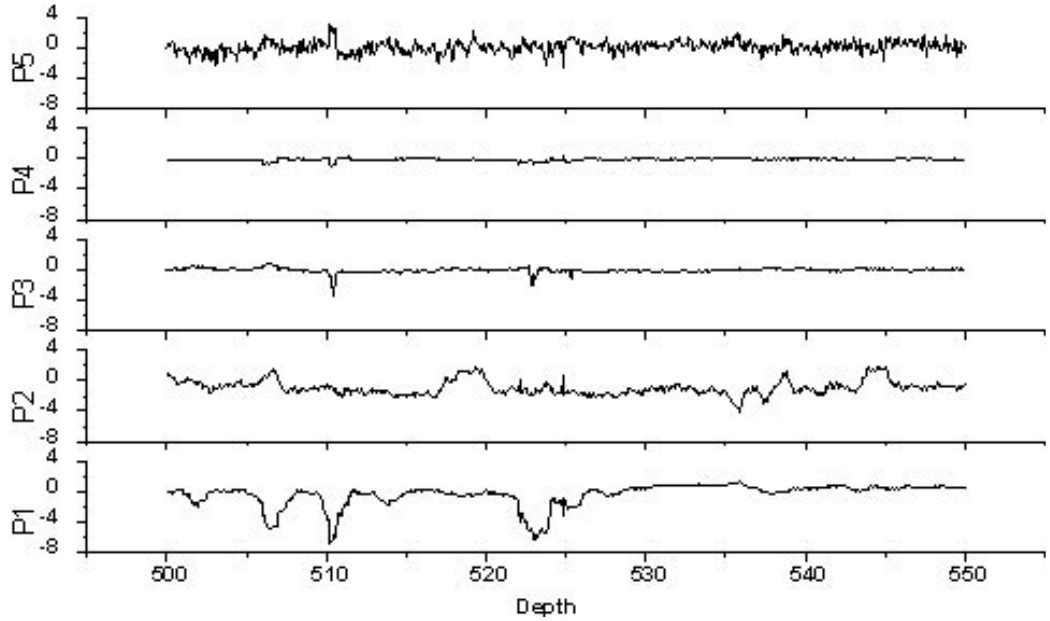

Figure 7. Principal components P1–P5 of borehole OL-KR04, depth 500–550 m.

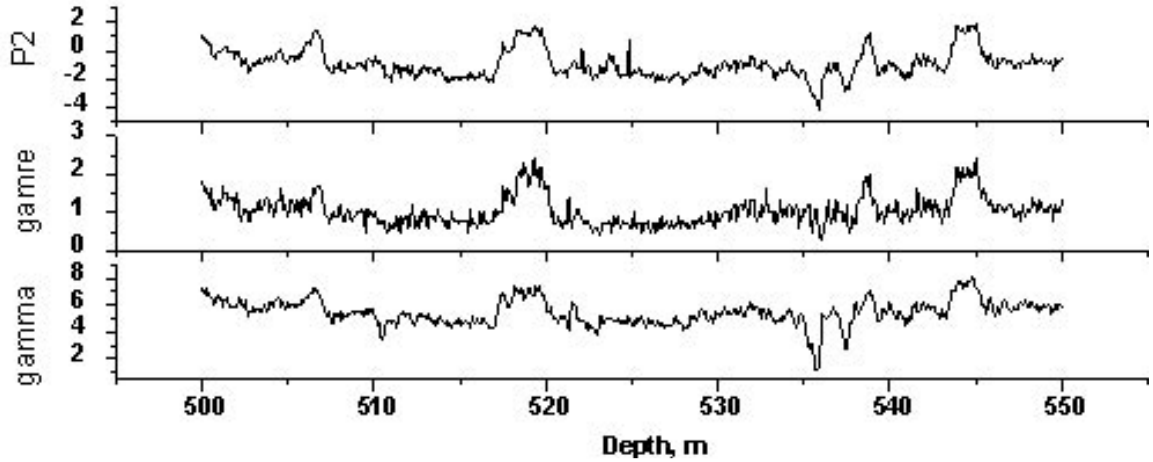

Figure 8. Principal component P2 and its main factors: gamma scattering (gamma, CPS) and gamma scattering relation of far and near detector (gamre).

between –4 and 4 in the borehole scale. The physical explanation of the anomalously low P2 values is decreased rock density due to the decreased specific density of rock (mineral composition), increased porosity, and increased volume of fractures. The gamma-gamma scattering method is typically used to determine rock type and porosity variations. The presented borehole section in Fig. 8 is anomalously low almost throughout, but it includes thin dense sections (granite) close to the depths of 506 m, 519 m, 539 m, and 544 m. The local minimum is detected close to the depth of 536 m (the section is not mentioned in the drilling report or further interpretations). Fracture detection using the component P2 is more problematic than using P1 due to geological facts. Rock density fluctuates in the Olkiluoto area where the rock mass is a mix of inhomogeneous rock clusters.

The factor P3 is composed mainly of the resistivity, resistance, and magnetic susceptibility data. P3's variation (Fig. 7) shows mainly thin penetrated sections in the borehole OL-KR04. The component detects two negative peaks between 500 m and 550 m as presented in Fig. 7 and 9. The peaks are clear and a "trigger limit" would be easy to determine. The behavior of P3 seems to imitate a resistance curve due to the noise-like variation in susceptibility and the rounded variation in the resistivity data (Fig. 9).

In the borehole scale, the behavior follows the susceptibility data because of four very anomalous sections close to the depths of 136 m, 390 m, 428 m, and 490 m. These short sections increase the importance of the susceptibility data in the calculations of the factor P3. However, the relatively short sections occupy a minor role in the borehole scale. The high values in the susceptibility data may be associated with the presence of magnetite minerals in the rock or fracture filling. The detection distance of susceptibility is restricted close to the borehole and does not show any large-scale variation in the property corresponding to the resistivity data.

The principal component P4 is produced mainly on the basis of the hydrological data. Typically, hydrological anomalies are located in open fractures, but the data is inconsistently not included in the calculation of P1. This interesting phenomenon in the PCA analysis is discussed in the next chapter.

The measurements of natural gamma radiation form the last principal component (P5). The measured background radiation is based on spontaneous disintegration of radioactive minerals. The most common radiogenic minerals in rock are uranium, thorium, and potassium. In comparison with the host rock, fracture zones differ slightly in their mineral content, but in the boreholes of Olkiluoto, the differences in the radioactive mineral content are not high enough for detecting fracture zones as sections of radiation minimum or maximum. The data has one very high peak in the borehole OL-KR04 at the depth of 764.7 m. The location is just below the fracture KR04_8R (Vaittinen et al. 2003). Probably

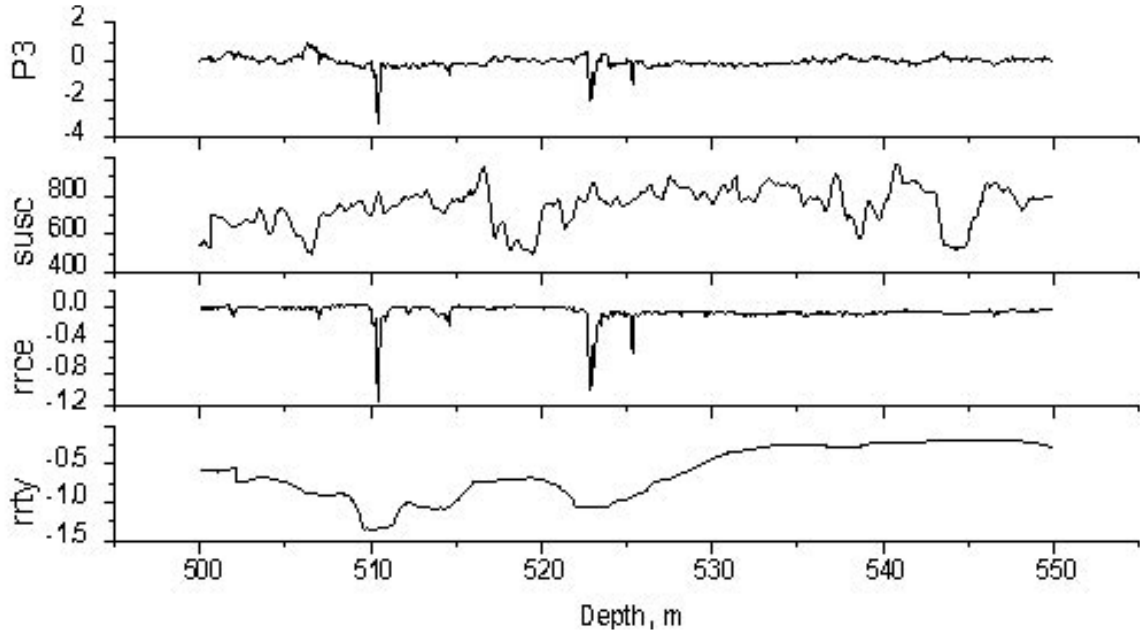

Figure 9. Principal component P3. The main factors are susceptibility (susc, SI), residual resistance (rrce, LOG Ohm), and residual resistivity (rrty, LOG Ohm-m).

a geological explanation for the measurement result exists but it is not dealt with in detail here.

5.2 Data restrictions

Some data modifications were performed prior to the PCA calculations in the previous chapter. An attempt was made to obtain data compatible with the analysis program (SPSS). The results show that the correlation between the hydrological parameters and P1 was unexpectedly missing. It was found that the hydrological data includes a few exceptionally high values. After making sure that these were the values behind the weak compatibility, necessary data modifications were carried out and the PCA results were recalculated.

Water flow and hydrological conductivity are interrelated. The principal component P4 is derived almost exclusively from these two data sets in the realized PCA calculation. The distribution of water flow varies between 10 ml/h and 0.36E6 ml/h. The mean of the measurements is 360 ml/h, but the median is only 20 ml/h. This highly skew distribution of the water flow values is caused by a relatively short but productive hydrological zone located close to the depth of 116 m. The measured high water flow values skew also the PCA process (the process works at its best when the data sets are normally distributed) and reduce the possibilities of identification of typical hydrological structures.

Winsorized distribution of water flow (wflow ≤300 m/s) leads to PCA results corresponding to those presented in Tables II and III, but improves the P4 presented in Fig. 7. Through winsorizing, the highest water flow values are reduced to 300 m/s (ca. 1.2% of the borehole length shows higher water flow than 300 m/s). Both hydrological features, large and small, (curve wflow in Fig. 11) produce recognizable responses in analyzes after winsorizing.

Hydrological conductivity is a very dynamic property of the rock mass. Similarly to the water flow data, the distribution of the hydrological conductivity data is skew and includes also numerous readings below the detection limit of the instrument. In the PCA, as well as in many other statistical methods, it is assumed that the data is normally distributed. The hydrological data includes 14% of zero values (i.e., values below the detection limit), but only few very high values. When the zero values are removed and the data distribution is presented in a logarithmic scale, the result fits much better with the normal distribution (Fig. 10).

The new PCA with the modified water flow and hydrological conductivity data produces only four main components instead of five. Water flow and

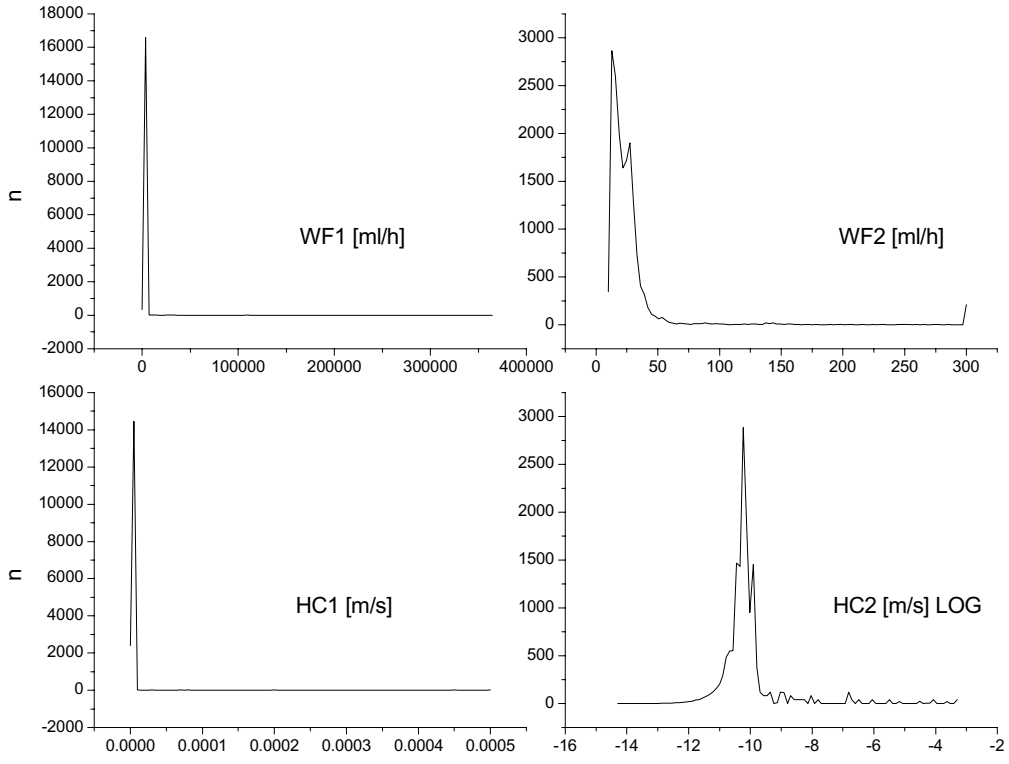

Figure 10. Histogram curve of water flow (WF, ml/h) and hydrological conductivity (HC, m/s). The curves WF1 and HC1 present original data distribution. The curve WF2 presents winsorized distribution of WF and the curve HC2 presents logarithmic HC without zero values.

hydrological conductivity move into the group of the first factor, P1. The correlation appears between the previously calculated P1 and the hydrological loggings. The caliber data loses its load in P1 below 0.5 and therefore it is no more in the group of the main components. The other factors P2, P3, and P5 do not change significantly. The new improved factor P1 explains 33% of all variation in the data set, but the four new components P1–P4 together explain 64% of all variation. The previous five factors P1–P5 in Table II covered 70% of the variation. The performed changes produce a stronger component P1, but a basically weaker PCA result.

5.3 Results of PCA

At present there are two alternatives of calculating the PCA and especially P1. In the first alternative, the original and unmodified water flow and hydrological conductivity together form almost alone the factor P4. In the second alternative, the PCA includes the modified water flow and hydrological conductivity data. The water flow and hydrological conductivity are integrated into P1. Factor Analysis of the modified data produces four main components from the 14 original data sets. The results after the axes optimization are collected into Table V. Below the factors P1–P4, the main components used and weightings are presented.

The principal component P1 includes the geological information RQD and fracture frequency. However, the sonic S-wave velocity data correlates better with the produced P1. If a single data set were to be selected to represent P1, it would be the S-wave (swave). Also, the visual example from the borehole depth of 500–550 m in Fig. 11 shows how the S-wave follows systematically the behavior of the factor P1.

The factor P2 is supported strongly by the gamma scattering data as shown in Fig. 8. The attenuation between the two detectors seems to have

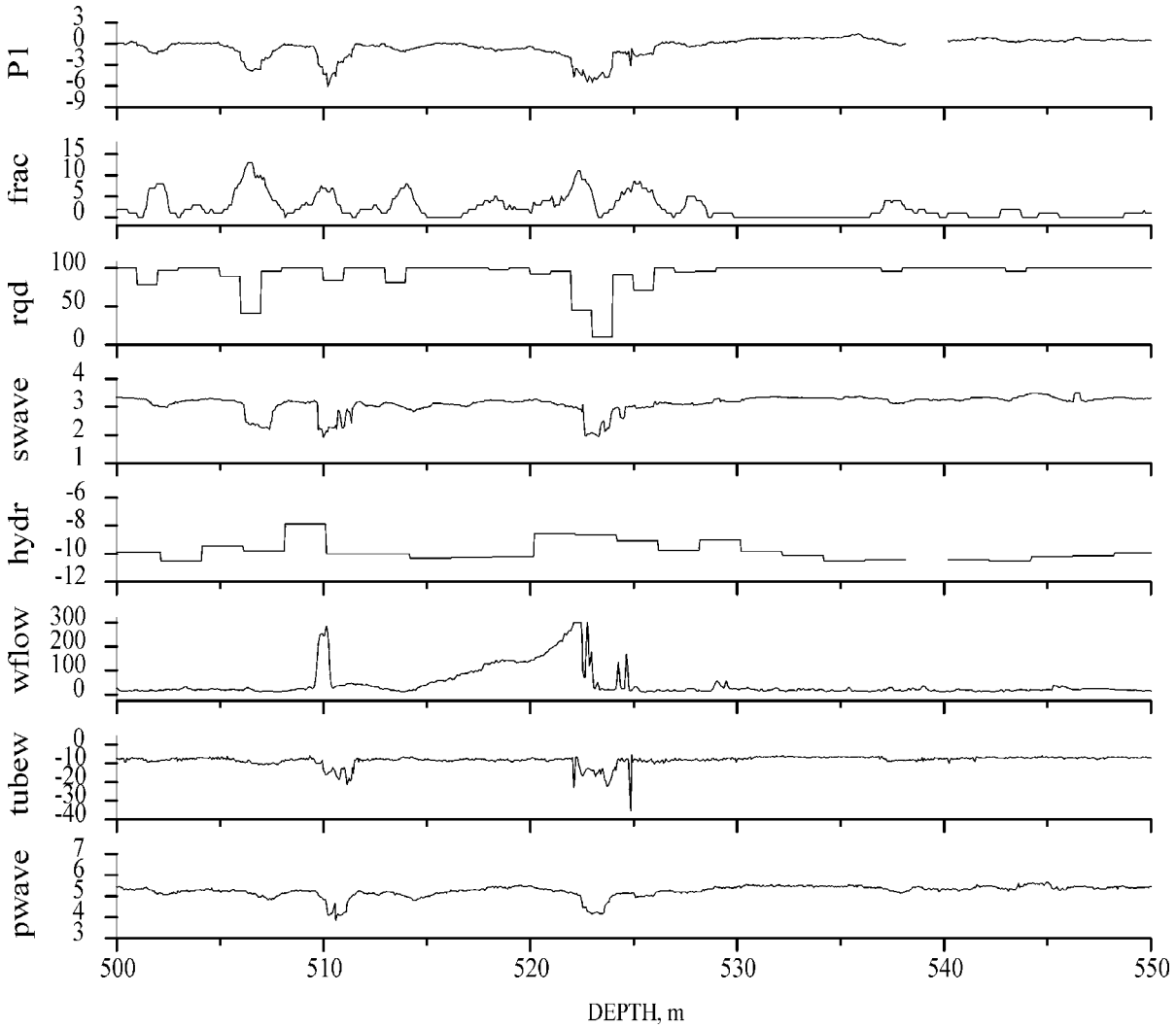

Figure 11. Principal component P1 and supporting borehole data in selected section of OL-KR04.

Table V. Factors P1 – P4, physical explanation, components and weightings.

P1 is formed of data that detects open (water filled) fractures	
S-wave velocity	0.845
RQD	0.780
P-wave velocity	0.751
fracture frequency	0.748
tube wave attenuation	0.670
water flow	0.548
hydraulic conductivity	0.500
P2 is formed of data that detects reduced rock density	
attenuation of gamma radiation	0.881
gamma-gamma scattering	0.878
P3 is formed of data that detects electrically conductive and magnetic minerals	
residual resistance	0.849
susceptibility	0.782
residual resistivity	0.675
P4 is formed of data that detects radioactive minerals	
natural gamma radiation	0.845

clearer variation and its support is slightly stronger than the gamma radiation of a single channel. If only a single data set were to be selected to represent P2, it would be the gamma-gamma scattering attenuation (gamre).

Residual resistance (rrce) would represent the factor P3, if only one data set were to be selected on the basis of the PCA results. The residual resistance and residual resistivity are compared visually in Fig. 12. Both methods detect the same electrically conductive zones, but the shapes of the anomalies are different. The geometry of the measuring electrodes (the long normal method) makes the resistivity (rrty) responses wide and soft. Single point resistance (rrce) has high resolution and very dynamic variation from point to point. Resistance anomalies outline sharply the borders of the electrically conductive zones. However, the "trigger limit" is not self-evident in this data. A high "trigger limit" picks only a narrow centre of conductive structures, but a low "trigger limit" rapidly increases the number of zones owing to the noise-type variation of low-level values.

Visually, it is noticed that a penetrated conductive layer or zone is equally detected by the resistivity as well as the resistance method. In the PCA analysis, the resistance data was more significant in the calculation of the principal component P3. To be more exact, the dynamic and sharp variation of the resistance is emphasized probably because of the small number of main parameters in the factor P3.

For fracture detection purposes, the resistance data has both advantages and disadvantages. The sharp variation helps to locate the borders of the different structures. However, the resistance data shows inconsistent variation that may be caused by a poor contact between the probe electrode and the borehole wall. Uncertainty with respect to an electrode contact does not prevent the detection of a conductive structure, but sometimes it cuts an anomaly to numerous short sections or peaks. It is quite possible, that a fracture filling close to a borehole wall is wiped away during drilling and the fracture filling is replaced by local fresh or

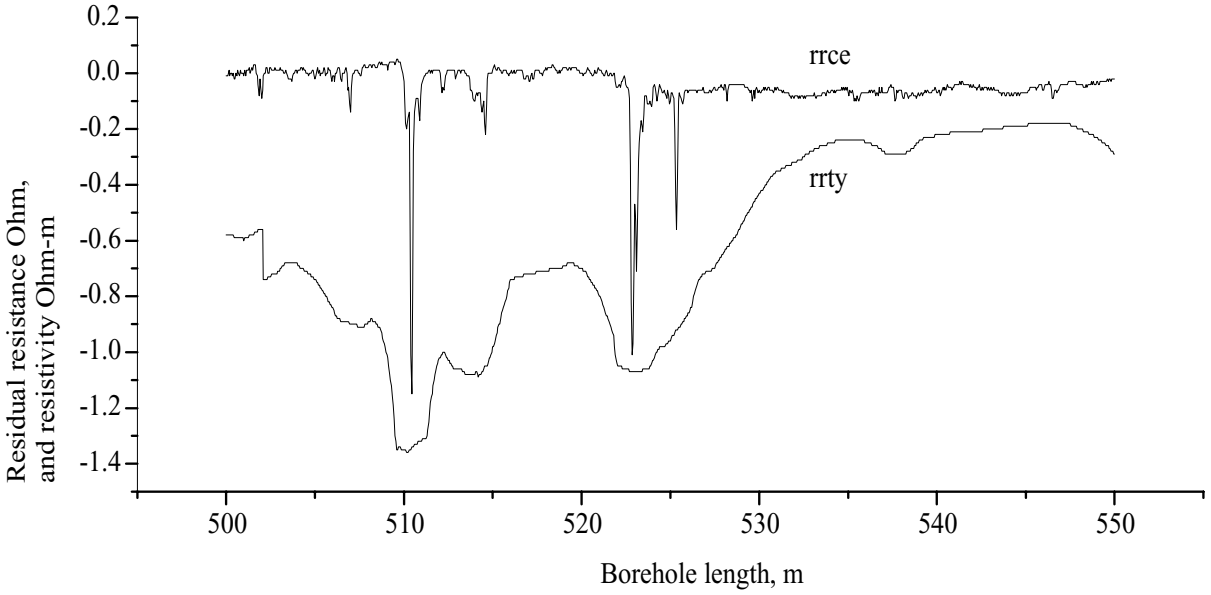

Figure 12. Residual resistance (rrce) and resistivity (rrty) in borehole OL-KR04, 500–550 m, logarithmic scale.

saline water with time. While the acoustic method locates an open fracture, the resistance method may indicate only a weak anomaly due to an incomplete contact. In the nearest vicinity of the open fracture, the electrode contact may be better again and the result may show lower resistivity.

The resistivity measurement is carried out with a long normal electrode array, which is widely used and a standard method in borehole loggings. The radius of investigation with a 1.6 m (64") probe electrode spacing is 1.0–2.3 m. The anomaly width is the thickness of penetrated conductive layer plus the probe electrode spacing 1.6 m (Poikonen 1983). As an example, the anomaly near the depth of 510 m presented in Fig. 12 is about 3 m wide and therefore the penetrated zone thickness is about 1.4 m. Compared to the other borehole methods, the resistivity method has a large investigation radius and it shows smooth variation. This kind of data is useful together with the S-wave velocity data that detects zone borders extremely sharply.

6 Identification methods

In fracture zone identification, the most valuable borehole logging data for the purposes of the PCA calculation and practical demands consists of

- S-wave velocity
- rock resistivity
- gamma–gamma scattering relation of far and near detector.

The presented data selection collects in-situ borehole information at different scales. The S-wave travels very close to the borehole wall from source to receiver. The variation in the S-wave velocity provides information on a volume that resembles a thin pipe around the borehole. The gamma–gamma measurement gives information on a larger volume resembling an ellipsoid. In this case, when the data is the relation of far-field and near-field results, the exact sphere of influence is more complicated than an ellipsoid, but certainly larger than the volume in the case of the S-wave measurement. The resistivity measurement with the electrode array used gives information on a varying volume around the probe. Strictly local conductive inclusions have an insignificant impact. However, a very thin, but extensive conductive plate will be detected easily.

One of the most important requirements of the PCA was to reduce the number of data sets. At present, the number of data sets is three and there is no reason to further combine them. The selected data set of three different methods represents the original information of 14 different data sets. The coverage of these three data sets is not perfect, but their usability is as good as possible.

For simplicity, the fracture detection method could be composed of two physically most suitable methods, namely the S-wave and resistivity. These methods have a direct connection with fracture properties whereas the gamma-gamma method logs indirect properties of fractures. Long-term fluid flow causes hydrothermal alteration that reduces rock density near fractures. Fracture volume has also some but typically minor influence on density.

6.1 Trigger limits

In a fracture detection process, the fracture zone is localized when a particular limit value in the data's properties is reached. It is important to set a correct "trigger limit" in order to be able to identify the correct relative number of fracture zones in a data. When parameter variation is normally distributed, the limit is easy to determine using the cumulative distribution function: for the highest 10% of the data, the trigger limit is 1.29, for the highest 5% it is 1.65, etc. The trigger limit 1.8 separates 3.6% of anomalous rock volume. Setting a "trigger limit" is only a mathematical task. In practice, the borehole data is not normally distributed and the trigger limit has to be set experimentally.

The data distribution of S-wave velocity is presented in Fig. 13. The given "trigger limit" of 3.1 km/s separates about 8.6% of the total length of the studied section (100–900 m) of OL-KR04. The separated values are typically much lower than the values in the main group of the distribution. The distribution supports the impression given by the visual profile interpretation: penetrated fracture sections are easy to define using the S-wave velocity data.

The residual resistivity data is broadly distributed. The given "trigger limit" separates about 17.8% of the total borehole length. Due to wide anomalies in the logging profiles as well as the wide data distribution, the resistivity data is not sensitive enough to localize the exact borders of the penetrated fracture zones. Especially, the narrow sections close to each other are difficult to

separate according to the resistivity data. However, the resistivity data localizes sections of electrical conductance outside the borehole.

6.2 Combination of data

The interdependence between the resistivity and S-wave data is presented in Fig. 14. The main group of the data represents the normal variation of intact rock. The "normal" resistivity value here is close to zero due to background / residual correction. S-wave velocity is about 3.2–3.3 km/s in solid rock. The main group of data points in Fig. 14 includes about 75% of all points.

Two different subgroups stand out in the data in Fig. 14. For both groups, the resistivity anomaly is almost one order of magnitude higher or more,

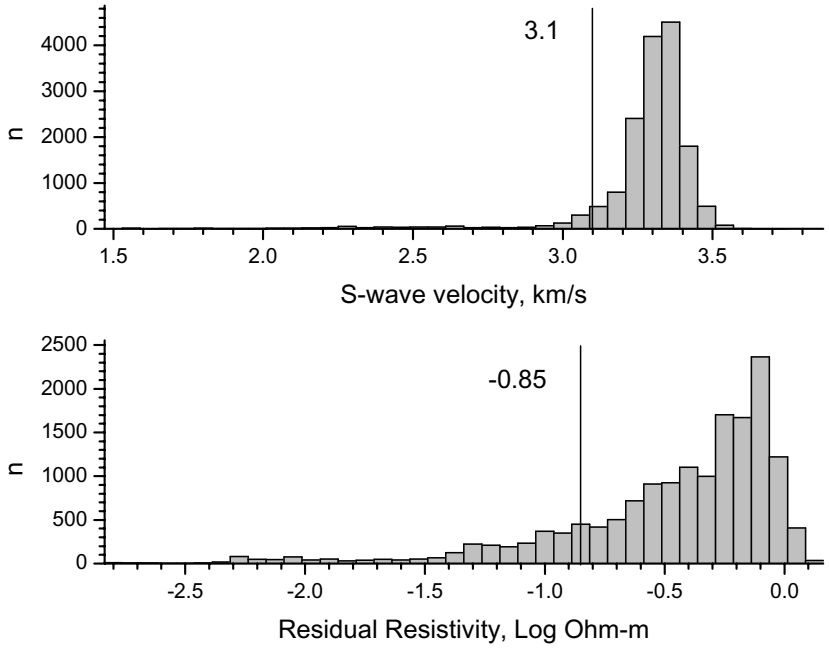

Figure 13. Distribution of residual resistivity and S-wave velocity with "trigger limits".

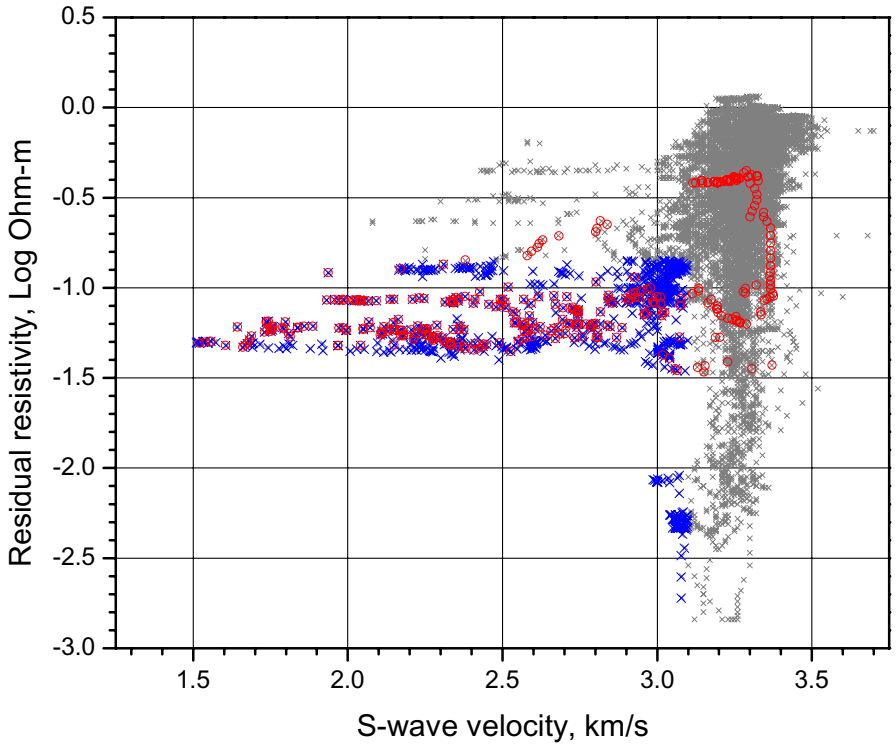

Figure 14. The dependence between S-wave velocity and resistivity data in the borehole OL-KR04. The number of samples in the borehole is 15,800. The blue crosses indicate the sample group where the conditions of the "trigger limits" are fulfilled (accounts for 5%). The red circles over grey and the blue crosses indicate stations inside the detected sections in Vaittinen et al. 2003.

which indicates mineralization or a fracture zone. One group shows a typical S-wave velocity of intact rock and therefore the group represents mineralization in intact rock. The other group with blue and red marks represents fracture zones where electrical conductivity is increased and open fractures are detected on the basis of low S-wave velocity values.

In Vaittinen et al. 2003, the fracture zone quantification found nine fracture zones penetrated by OL-KR04. The detected crushed zones, fractured zones, and hydrological features are presented in Table VI. Data points located inside the detected zones are marked with red circles (n=375) in Fig. 14 (excluding two sections above the depth of 100 m). A majority (n=240, 64%) of the zone points have values within the "trigger limits". The result shows that there is evident compatibility between the simple detection method based on the two borehole logging methods and the in situ detection system.

The blue crosses without red circles (n=425) in Fig. 14 represent potential fracture zone points outside the named structures in Vaittinen et al. 2003. There are various reasons to why these points are not taken into the fracture zone grouping. Sometimes a detected section has been too short, sometimes the applied methods of a detection system have not found any critical properties, etc. However, these points have physical characteristics that require attention.

The red circles (Fig. 14) outside the "trigger limits" represent intact rock inside a fracture zone. The reason for the existence of discordant points is obvious. Also in Vaittinen et al. 2003, the zone definition is based purely on hydrological conductivity measurements. Because of the 2 m long packer distance of the measuring probe, the shortest section length is 2 m. However, a few important borehole sections have also been measured using shorter sampling distances, but the minimum fracture zone length is still 2 m in Vaittinen et al. 2003. The detected zone includes a hydrological conductive fracture as well as other rock close to the fracture.

6.3 Identification in OL-KR04

The results obtained from the borehole OL-KR04 through the application of the residual resistivity and S-wave velocity data with "trigger limits" are presented in Fig. 15 and 16. A borehole section of 100–500 m in depth is shown in Fig. 15. The curve on the left in the Figure is the S-wave velocity with the used "trigger limit" (3.1 km/s). The detected borehole sections with lower velocity values are presented with red colour in the middle of the figure. The other curve represents residual resistivity with the used "trigger limit" (10E–0.85 Ohm-m). The sections of low resistivity are shown with blue pillars in the middle of the figure. Sections where both methods show values below the "trigger limit" simultaneously are marked with black pillars. For comparison, the results of Vaittinen et al. 2003 (Table VI) are also presented in the same figure (Fig. 15 and 16). The zones are presented with green section marks.

Table VI. Zones of OL-KR04 (Vaittinen et al. 2003).

Number	Name	Depth	Classification
1	KR04_1H (R45)	59.4 – 61.4 m	Hydraulic feature
2	RH19A	80.5 – 84.1 m	Fracture zone
3	RH19B	115.6 – 117.6 m	Fracture zone
4	KR_04H	305.9 – 307.9 m	Hydraulic feature
5	RH20A	312.5 – 316.7 m	Crushed zone
6	RH20B	365 – 367 m	Crushed zone
7	RH04_7R	522.22 – 524.22 m	Crushed zone
8	RH21	756.7 – 764.2 m	Crushed zone
9	KR04_9H	862.7 – 864.7 m	Hydraulic feature

The result of the applied geophysical detection methods includes several thin fractures (Fig. 15 and 16). This corresponds exactly to natural variation. The fracture zones are not straight plates without branches or occasional local variation. The paper of Front and Okko (1994) presents plenty of illustrations of natural fracture variation collected from literature. The complex geology of the Olkiluoto area controls all fractures and the details of fracture structures are obviously also difficult to understand or model. These sections are located sometimes close to each other and sometimes there are wide areas without notable fractures.

The detected fracture zones according to the S-wave velocity and resistivity data are located in four depth regions in the borehole OL-KR04 (the studied depth range lies at 100–900 m). The first weakness zone is located between the depths of 110 m and 140 m. The low resistivity indicates mineralization in the foot of the section. The other three zones are at the depths of 310–405 m, 505–525 m,

and 755–790 m. There are also two solitary thin sections detected at 271 m and 489 m. The section located deeper is connected to an electrically highly conductive structure. The weakness zone close to the 500 m depth may be interconnected with this geological feature as well.

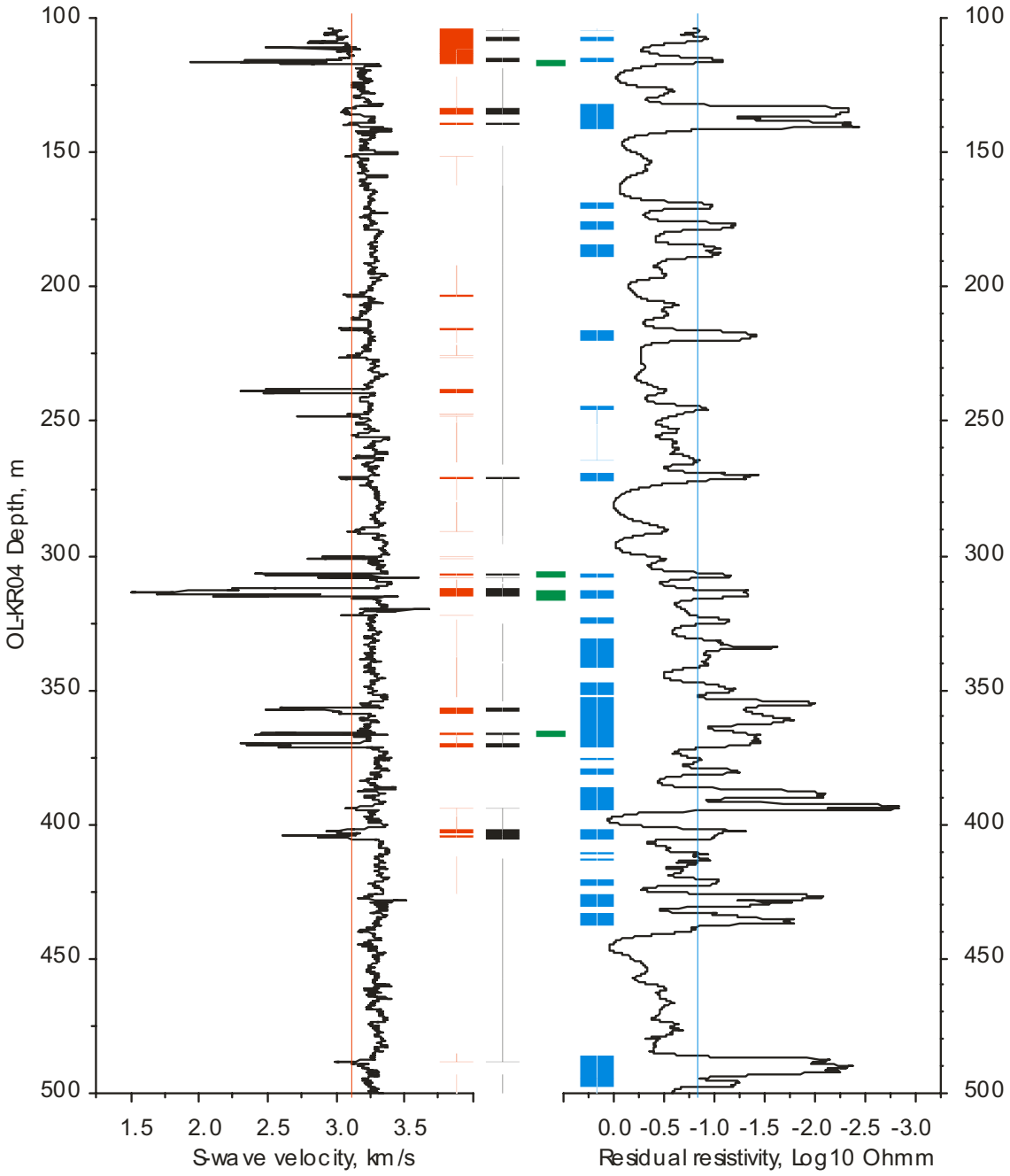

Figure 15. Detected sections of borehole OL-KR04 between 100 m and 500 m depth. The trigger limit of the S-wave velocity is 3.1 km/s. Sections with low S-wave velocity are presented with red colour. The trigger limit of the logarithmic residual resistivity is –0.85 Ohm-m. Sections of low resistivity are presented in blue colour. The black colour presents findings where both the S-wave velocity and resistivity are low. The green sections present fracture zones determined in Posiva Ltd's geological model, version 2003/1.

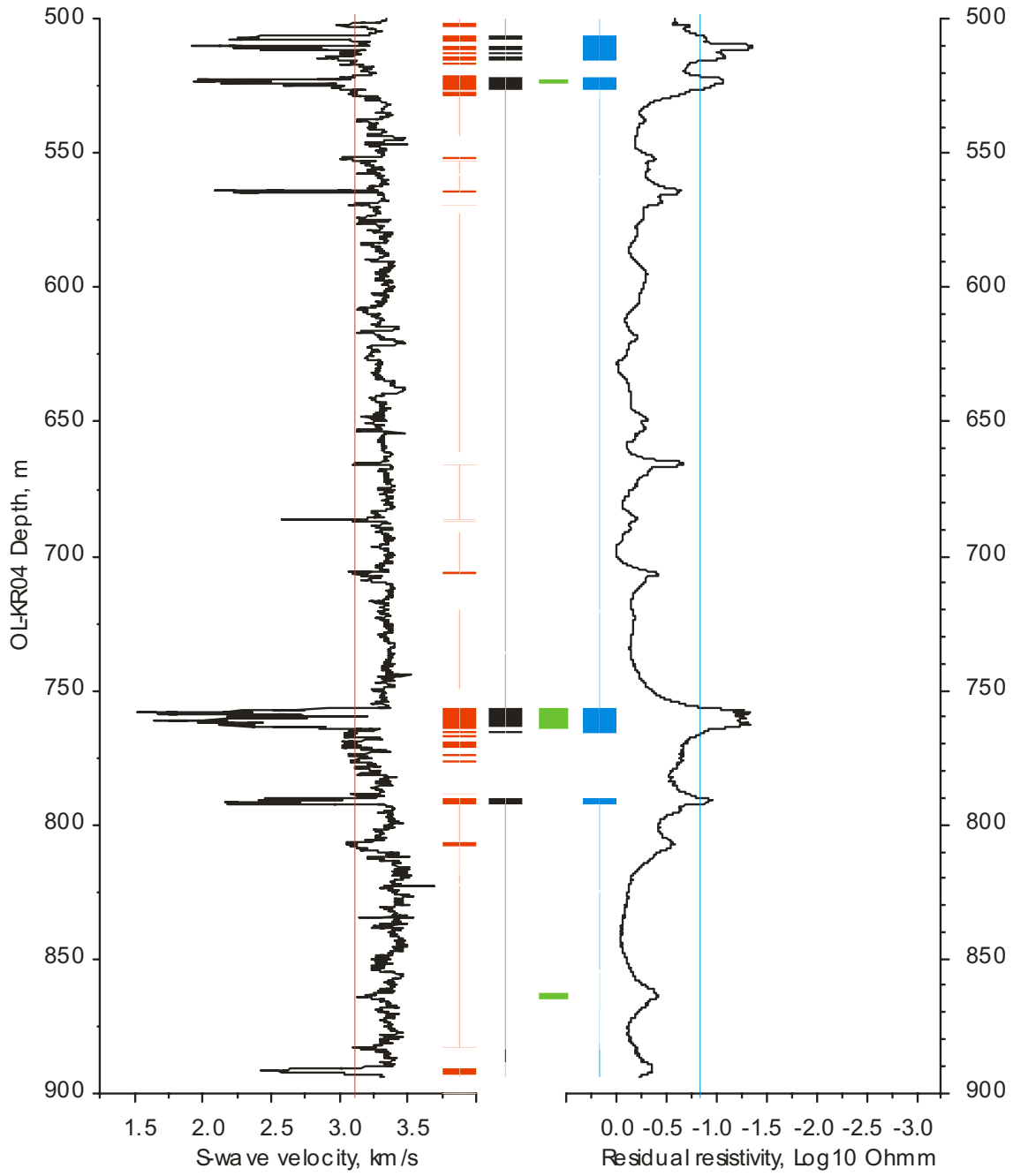

Figure 16. Detected sections of borehole OL-KR04 between depths 500 m and 900 m.

6.4 Method combination

The visual estimation of a drill core produces a quick classification of the different kinds of penetrated zones and penetrated intact rock mass. Hydraulic features (WA5, WA6), fractured zones (ZONE), and zones of slices (SLICES) could be pointed out on the basis of the outward appearance of the drilling samples and the results of hydrological measurements. The visually determined zones of OL-KR04 are presented in Fig. 17.

Fracture zone identification is based on observed or measured fracture zone characteristics. The most important data source is the core sample. Hydrological conductivity logs form other essential data. It is possible to build a fracture identification system on these two data sets. Increased hydrological conductivity forms clear evidence for the determination of fluid flow paths with or without additional information on rock quality. Equally, a crushed zone without high values of hydrological conductivity is a sign of poor rock quality. The section has possibly no continuity or it is filled with clay or other material that prevents fluid flow.

The classification factor "ZONES" is based on the visual inspection of the drill core, RQD- values, fracture density, and other observations (to avoid

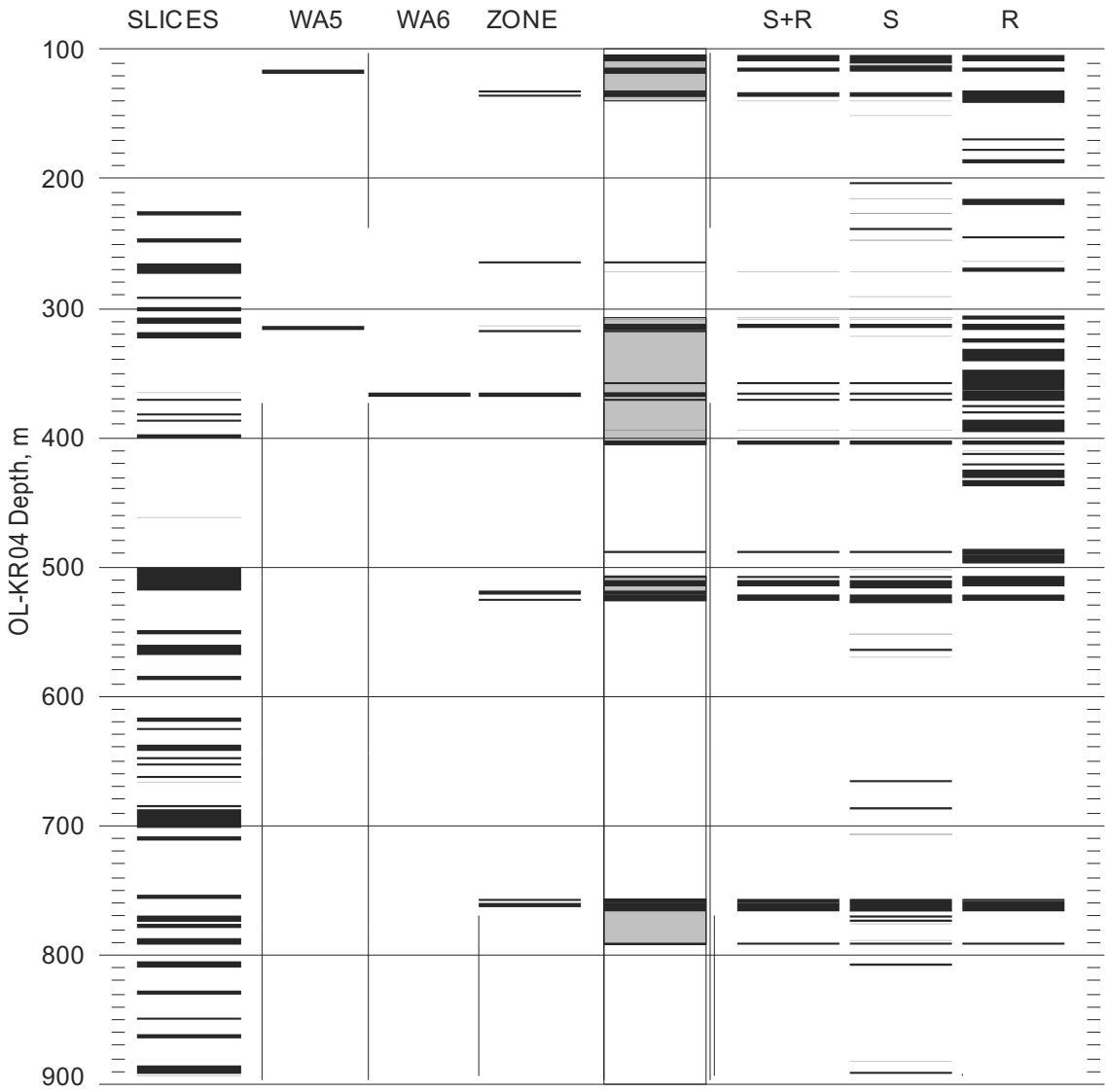

Figure 17. Results from different fracture zone identification methods. WA5 shows sections of hydrological conductivity with over 1·10E–5 m/s and WA6 shows the corresponding values exceeding 1·10E–6 m/s. ZONE shows the sections of poor rock quality and SLICES shows the densely fractured zones including slickensides. S+R show the shared result of low S-wave velocity (S) and low resistivity (R). The combination of hydrological features, zones, and geophysical identification is presented in the middle with grey interpreted section marks.

Table VII. Methods of the simple identification system.

	METHOD	IDEA	TYPE
1	Core sample	Visual interpretation of fractures and crushed zones	Crushed zone
2	Hydrological conductivity	Fractures in connection with an absorptive volume increases hydrological conductivity	Hydrological feature
3	S-wave velocity	Water in open fractures prevents S-wave propagation	Important fracture characteristics
4	Resistivity	Increased water and mineral content reduces electrical resistivity	

technical artifacts) from the original drilling reports. It notices only clearly distinct crushed zones.

The classification factor "SLICES" is mainly based on the visual inspection of the drill core. The idea is to identify sections of exceptionally dense fracturing on the basis of the drill core's external appearance without using any particular units of measurement. It is a proportional unit, dependent on the overall fracturing density of the analyzed borehole. It also notices longitudinal fracturing. This classification has been developed and tested at STUK to allow for an independent and alternative approach. It has been applied to almost all the drillholes of Olkiluoto.

Additional in-situ borehole data confirms, but also completes, the restricted interpretation of the core and hydrological data. The S-wave data gives accurate locations of water filled fracture sections. The resistivity measurement identifies electrical connections outside the borehole walls including a fracture net that contains saline or mineral-bearing water. Owing to different kinds of electrical conductors, the resistivity data is usable for fracture detection only when it is coupled with another data set. The local saline groundwater has a resistivity of about 0.1–5 Ohm-m which is comparable to the local mineralization. Due to high rock resistivity (about 5,000–10,000 Ohm-m) in the area, the resistivity contrast between an open fracture and the host rock is high enough for a reliable detection.

The four methods in Table VII complete the simple and fast fracture zone identification system. Generally, these four methods are sensitive to several different kinds of rock characteristics and physical properties. However, core sample information may show the highest correlation with S-wave velocity because of the small S-wave penetration.

The first two fracture section types have been introduced earlier: crushed rock (TYPE 1) and hydrological feature (TYPE 2). The third type is the fracture zone of important fracture characteristics identified by the seismic and electric method (TYPE 3). This section type shows characteristics that cannot be overlooked in borehole analysis. The rock characteristics cause the measured borehole data to exceed the trigger limits.

In practice, the "trigger limit" controls the sensitivity of a section's identification. With loose "trigger limits", the number of sections and their proportion of the borehole length is high. With tight values, only the most important sections are identified. The selected "trigger limits" presented in Fig. 14–16 are considerably tight.

7 Conclusions

In the site investigation and rock characterization of nuclear waste disposal, the most important task is to localize intact rock volumes. In practice, the highly fractured zones form the borders of less fractured areas. Borehole and surface information is used to detect the important fracture zones and, in addition, to characterize the hydrological properties, direction, and extension of these zones.

The work focuses on the borehole data of OL-KR04 with a view to develop a new simple method of identifying fracture zones. First, the available borehole data is interpolated to a 0.05-m point distance. The principal component analysis is carried out in order to combine several physically different new factors for the purpose of explaining variation in the original data. The most important factor explains ca. 30% of all variation. Noise and data with weak correlation with other data explains ca. 36% of all variation.

The S-wave velocity data fits best with the combined first principal component and shows simultaneously strong correlation with water bearing fractures. The step-like variation of the S-wave velocity data forms practical data for the localization of fracture zone borders. Other essential factors are hydrological conductivity as well as the direct analysis of crushed sections of the drillcore. Rock resistivity is a parameter for enlarging investigation distance from the borehole to the surrounding media.

The combination of the resistivity and S-wave velocity data is based on physical facts. The aim is to obtain as useful information as possible taking advantage of the short measurement periods available during the excavation of the characterization tunnel and ONKALO. The measurements are quick to carry out and the method requires only simple interpretation using the "trigger limits". The method accepts thin and thick fracture sections and forms an interpretation that corresponds to natural variation and complexity.

Weakness zones below 100 m in the borehole OL-KR04 are located by the developed method at the borehole distances 110–140 m, 310–405 m, 505–525 m, and 755–790 m. These sections are not continuously crushed or densely fractured, but they form potential weakness zones. When characterizing intact rock volumes for repository, a safety distance has to be added outside the detected zones.

Presented fracture identification method could form a basement for alternative geological modelling comparable to Posiva's model. Naturally, the purpose of this simple approach is not to compete with other models, rather to look at the same data from different point of view. Probable differences between models may bring up discussion about reasons behind the differences. Hopefully this results model improvement in repository work in long term.

For complete alternative model the fracture identification method is just a beginning. The first logical step forward is to adapt the method to all boreholes at the site. Next phase is connecting fracture zones between boreholes. In that part of modelling all available direction-dependent data is needed. Fracture directions, geological structures, VSP-interpretations and numerous other observations and conclusions should be applied.

References

Gardemeister, R., Johansson, S., Korhonen, P., Patrikainen, P., Tuisku, T. and Vähäsarja, P., 1976. The application of Finnish engineering geological bedrock classification (in Finnish). Espoo, Finland: Technical Research Centre of Finland, Geotechnical laboratory. 38 p. Research note 25.

Front, K. and Okko, O., 1994. Fractures and fracture zones in conceptual modelling – geological and geophysical considerations. Work report PATU-94-27e. VTT Communities and Infrastructure Rock and Environmental Engineering. 70 p.

Harman, H. H., 1967. Modern Factor Analysis. Second Edition. University of Chicago Press.

Jokinen, J. and Jakobsson, K., 2002. Focused modelling of bedrock fracture zones in Olkiluoto. Nuclear Waste Disposal Research, Report YST-111.

Korhonen, K-H., Gardemeister, R., Jääskeläinen, H., Niini, H. and Vähäsarja, P., 1974. Engineering geological bedrock classification (in Finnish). Espoo, Finland: Technical Research Centre of Finland, Geotechnical laboratory. 78 p. Research note 12.

Korkealaakso, J., Vaittinen T., Pitkänen, P., and Front, K., 1994. Fracture zone analysis of borehole data in three crystalline rock sites in Finland – The principal component analysis approach. VTT Communities and Infrastructure. YJT-94-11.

Niinimäki, R., 2004. Core drilling of pilot hole OL-PH1 at Olkiluoto in Eurajoki 2003-2004. Working Report 2004-05. Posiva Oy, Helsinki. 33 p.

Paananen, M., 2001. Interpretation of properties and occurrence of fracture zones in repository conditions. Geological Survey of Finland, Nuclear Waste Disposal Research, Report YST-103 (in Finnish, abstract in English).

Poikonen, A., 1983. Application of electrical and thermal borehole loggings to structural and hydrological investigations of crystalline bedrock. Valtion teknillinen tutkimuskeskus, Tutkimuksia – Statens tekniska forskingscentra, Forskningsrapporter – Tecnical Research Cetre of Finland, Research Reports 212. Espoo. 80 p. + app. 8 p.

Rautio, T., 1995. Drillings at Olkiluoto in Eurajoki 1995, Extension of the Borehole OL-KR4. Suomen Malmi Oy. Working Report PATU-95-46 (in Finnish, abstract in English), 20 p + appendices and color figures of core samples.

Reyment, R. A. and Jöreskog, K. G.,1993. Applied Factor Analysis in the Natural Sciences. Cambridge University Press.

Tammisto, E., Lehtimäki, T., Palmén, J., Hellä, P. and Heikkinen, E., 2002. Fracture mapping from Olkiluoto borehole image data, 2001. Working Report 2002-22. Posiva Oy, Helsinki. 109 p.

Vaittinen, T., Saksa. P., Nummela, J., Palmén, Hellä, P., Ahokas, H. and Keskinen, J., 2001. Bedrock model of Olkiluoto site, revision 2001/1. Olkiluoto, Finland: Posiva Oy. Working report 2001-32 (in Finnish, abstract in English), 190 p.

Vaittinen, T., Ahokas, H., Heikkinen, E., Hellä, P., Nummela, J., Saksa, P., Tammisto, E., Paulamäki, S., Paananen, M., Front, K. and Kärki, A., 2003. Bedrock model of the Olkiluoto site, version 2003/1. Working Report 2003-43. Posiva Oy, Helsinki. 124 p.